ARTICLE

OBC
www.rsc.org/obc

Ab initio study of the binding of Trichostatin A (TSA) in the active site of Histone Deacetylase Like Protein (HDLP)

Kenno Vanommeslaeghe,*[a] Christian Van Alsenoy,[b] Frank De Proft,[c] José C. Martins,†[d] Dirk Tourwé[a] and Paul Geerlings[c]

[a] *Vrije Universiteit Brussel, Organic Chemistry Group, Pleinlaan 2, B-1050 Brussel, Belgium. E-mail: Kenno.Vanommeslaeghe@vub.ac.be; Fax: +32 2 6293304; Tel: +32 2 6293300*

[b] *Universiteit Antwerpen, Structural Chemistry Group, Universiteitsplein 1 C2.20, B-2610 Wilrijk, Belgium*

[c] *Vrije Universiteit Brussel, General Chemistry Group, Pleinlaan 2, B-1050 Brussel, Belgium*

[d] *Vrije Universiteit Brussel, High Resolution NMR Centre, Pleinlaan 2, B-1050 Brussel, Belgium*

Received 1st May 2003, Accepted 30th June 2003
First published as an Advance Article on the web 15th July 2003

Histone deacetylase (HDAC) inhibitors have recently attracted considerable interest because of their therapeutic potential for the treatment of cell proliferative diseases. An X-ray structure of a very potent inhibitor, Trichostatin A (TSA), bound to HDLP (an HDAC analogue isolated from *Aquifex aeolicus*), is available. From this structure, an active site model (322 atoms), relevant for the binding of TSA and structural analogues, has been derived, and TSA has been minimized in this active site at HF 3-21G* level. The resulting conformation is in excellent accordance with the X-ray structure, and indicates a deprotonation of the hydroxamic acid in TSA by His 131. Also, a water molecule was minimized in the active site. In addition to a similar deprotonation, in accordance with a possible catalytic mechanism of HDAC as proposed by Finnin *et al.* (M. S. Finnin, J. R. Donigian, A. Cohen, V. M. Richon, R. A. Rifkind and P. A. Marks, *Nature*, 1999, **401**, 188–193), a displacement of the resulting OH^- ion in the active site was observed. Based on these results, the difference in energy of binding between TSA and water was calculated. The resulting value is realistic in respect to experimental binding affinities. Furthermore, the mechanism of action of the His 131–Asp 166 charge relay system was investigated. Although the Asp residue in this motif is known to substantially increase the basicity of the His residue, no proton transfer from His 131 to Asp 166 was observed on binding of TSA or water. However, in the empty protonated active site, this proton transfer does occur.

Introduction

Inhibitors of HDAC (histone deacetylase) have an antifungal, antiprotozoal and phytotoxic activity[1] and are potentially important therapeutics in the treatment of various cancers.[2,3,4] In addition, promising *in vitro* results have been reported concerning a wide variety of other diseases, such as fibrotic diseases,[5] including liver fibrosis,[6] an important cause of death in Western society, autoimmune[7] and inflammatory[8] diseases and polyglutamin disease.[9,10] Also, they have been shown to inhibit dedifferentiation in cell cultures.[11] TSA (**1**) (Fig. 1) was the first potent HDAC inhibitor discovered.[12] Although the synthesis[13] of the compound itself is too complex to allow economical pharmaceutical use and its metabolization is too rapid,[14] it is an interesting lead compound for the development of HDAC inhibitors as it features a high affinity for HDAC[15] and a small size in comparison with other natural HDAC inhibitors like Apicidin[16] (**3**) and Trapoxin[17] (**4**). For example, the TSA analogue Suberoylanilide hydroxamic acid[18] (SAHA) **2** is in Phase I clinical trials.[3]

† *Present address*: Universiteit Gent, NMR and Structural Analysis Unit, Krijgslaan 281 S4, B-9000 Gent, Belgium.

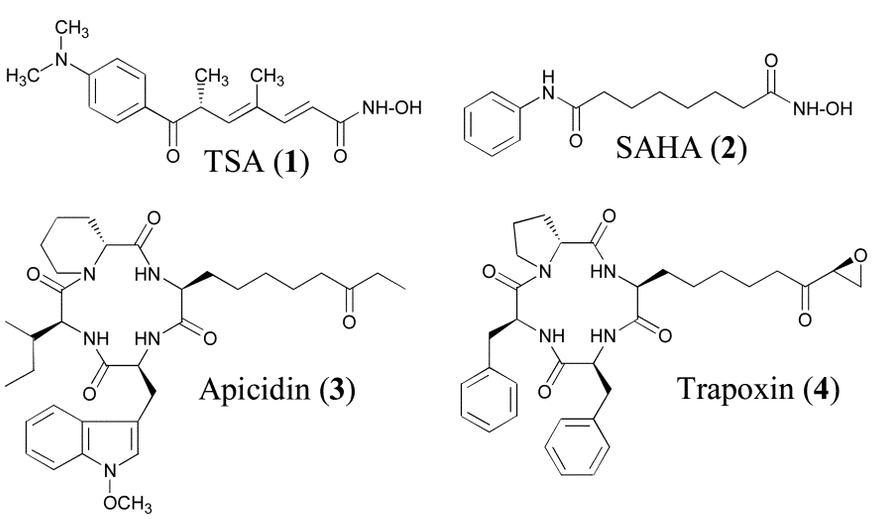

Fig. 1 Some known HDAC inhibitors.

DOI: 10.1039/b304707e

Recently, efforts have been made to model the interaction of TSA analogues with HDAC using empirical methods.[15,19,20,21,22] However, it is still unclear why some series of similar inhibitors display large differences in binding affinity.[23] This may be due to the fact that, except for the chelation of the catalytic zinc ion by the hydroxamic acid, it is difficult to identify common specific interactions between the enzyme and its inhibitors. For example, in the X-ray structures of TSA (**1**) and SAHA (**2**) in complex with HDLP,[24] little evidence for polar interactions can be found, except for the chelation of the zinc atom by the hydroxamic acid. Moreover, hydroxamates lacking an aromatic group show a smaller binding affinity than their counterparts having an aromatic ring,[25,26] which might indicate that interactions involving π–electron clouds play an important role. Unfortunately, such interactions are more difficult to quantify and are not included in MM force fields. These considerations led us to the use of a quantum mechanically based approach to gain insight into these interactions, as we recently also applied to other biomolecular systems.[27]

An active site model for HDLP was constructed based on the abovementioned X-ray structures.

At the computational level, Hartree–Fock calculations were performed with a 3-21G* basis set. Despite the fact that DFT calculations are very cost-effective and would presumably yield more accurate results, they are currently still computationally prohibitive for a minimization on a model of this magnitude. The semi-empirical models AM1 and PM3 were also considered for their low computational cost, but rejected because both yielded unsatisfactory results when minimizing TSA in vacuum (*vide infra*).

Using the chosen *ab initio* method, TSA and water were minimized in this active site model, providing insight into the mode of enzyme–inhibitor interaction.

Theory and computational details

Preparation of the X-ray structure

To the HDLP/TSA complex obtained from the Brookhaven Protein Data Bank[28] (entry code 1C3R, resolution: 2.1Å), hydrogen atoms were added and minimized, using the ESFF forcefield[29] as implemented in the Insight II software.[30]

Ab initio energy minimizations

All optimizations were gradient based, carried out at the HF/3-21G* level until all Cartesian forces on non-fixed atoms were below 0.001 mdyn. For these calculations, the *ab initio* program BRABO[31] was used. This program uses the multiplicative integral approach (MIA),[32] which yields a substantial reduction in required CPU-time without affecting the accuracy of the results, especially for large systems, the geometry determination of Crambin being a prominent example.[33] The total time taken for the minimizations of TSA in the active site of HDLP was about 57 days on an alpha EV6.8CD (1001 MHz, 2Gflops) CPU.

Calculation of BSSE corrected energy of interaction

The interaction energy was calculated using the counterpoise method[34] for correcting the basis set superposition error (BSSE). In this type of calculation, the difference is made between the total energy of the complex $E^{EL}_{bind}(EL)$, the energy of the ligand in the presence of the basis sets of the enzyme $E^{EL}_{bind}(L)$ and the energy of the enzyme in the presence of the basis sets of the ligand $E^{EL}_{bind}(E)$. This difference is the interaction energy between enzyme and ligand in their respective binding conformations. Then, to assess the energetic cost to reach this binding conformation, the parts that previously were not fixed in the active site, were minimized in the absence of the ligand to yield $E^{E}_{min}(E)$, and the resulting total energy was compared to the energy of the binding conformation $E^{E}_{bind}(E)$. The energy of the binding conformation of TSA $E^{L}_{bind}(L)$ was likewise compared to the energy of the absolute minimum of a MMFF94 systematic conformational search, re-minimized at 3-21G* level, $E^{L}_{min}(L)$. This procedure can be summarized as following:

$$\Delta E_{\mathbf{binding}} = [E^{EL}_{bind}(EL) - E^{EL}_{bind}(E) - E^{EL}_{bind}(L)] + [E^{E}_{bind}(E) - E^{E}_{min}(E)] + [E^{L}_{bind}(L) - E^{L}_{min}(L)]$$

where $E^{C}_{B}(A)$ denotes the energy of molecule A at geometry B and with the basis sets of C, A and C being either the enzyme E, the ligand L or the complex EL.

As mentioned in the introduction and further discussed in 'results and discussion', a proton transfer from the ligand to the active site was observed during the minimizations. To execute the subsequent BSSE procedure, a choice had to be made as to whether this proton was to be counted as part of the ligand or of the active site. If the former would be chosen, the hydroxamic acid OH bond would measure 1.79 Å and one of the OH bonds in water 3.65 Å. Since an RHF calculation cannot be expected to yield accurate energies under these circumstances,[35] the mobile proton was counted as part of the active site. However, as a result of this choice, it is necessary to incorporate deprotonation energies into the calculation of the binding energy of TSA relative to water. For reasons of consistency, these energies of deprotonation were calculated in vacuum, using the same BSSE procedure as mentioned above. Taking into account the fact that a single proton does not possess an electrostatic energy, this procedure is reduced to the following form:

$$\Delta E_{\mathbf{prot}} = [E^{HB}_{HB}(HB) - E^{HB}_{HB}(B^-)] + [E_{\mathbf{HB}}{}^{\mathbf{B}^-}(B^-) - E^{\mathbf{B}^-}{}_{\mathbf{B}^-}(B^-)]$$

Then, the process depicted in Fig. 2 was considered.

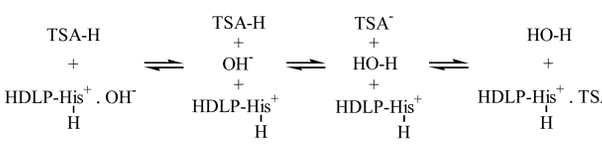

Fig. 2 Formal mechanism for estimating the binding energy of TSA, relative to water.

The energy difference associated with this process is:

$$\Delta\Delta E_{tot} = \Delta E_{\mathbf{binding}}(TSA^-) - \Delta E_{\mathbf{prot}}(TSA^-) - \Delta E_{\mathbf{binding}}(OH^-) + \Delta E_{\mathbf{prot}}(OH^-)$$

Results and discussion

Preliminary semi-empirical study

The X-ray structure of TSA was minimized both at the AM1 and the PM3 level. However, neither of these minimizations resulted in a planar structure as would be expected both from the resonance forms depicted in Fig. 3 and from the X-ray structures of TSA[36] and TSA bound to HDLP.[24] This motivated the choice of an a*b initio* method for the minimization of TSA in the active site.

Delineation of the active site model

The X-ray structure, prepared as discussed in "Theory and computational details", was stripped of its water molecules and all residues outside a radius of 4.5 Å around TSA were deleted. To this crude active site model, Asp 166 and Asp 173 were reintroduced, because they are both part of His–Asp charge relay systems involving His131 and His132 in the active site and thus probably play important roles in binding and catalysis. Then, Asn 20 was removed because this surface residue is outside the reach of TSA's dimethylaminobenzoyl terminus,

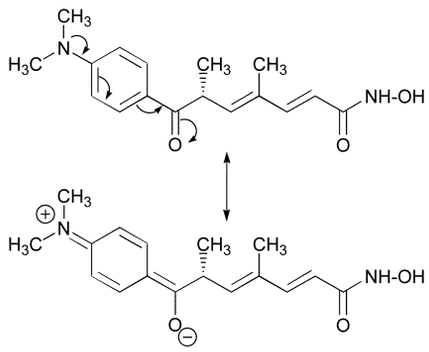

Fig. 3 Resonance structures of the "dimethylamino-terminal" π-system.

and the polar side chain points away from TSA's capping group. Phe 200 was removed because TSA doesn't make any contact with it and molecular mechanics conformational studies on TSA and comparable molecules[15,19,20,21,23] indicate that this region of the protein surface cannot be accessed by the capping group. For the same reason, His 21 was replaced by a Gly residue, retaining its main chain because its amide group is close enough to TSA's dimethylamino moiety to form a polar interaction. Gly 295 was removed because the nearest part of TSA, the hydroxamic acid function, chelates the Zn^{2+} ion and cannot get close enough to form nonpolar interactions. Finally, Ile 167 and Ile 169 were replaced by Gly residues because they are on the inside of the "bulk" protein and their side chains point away from the active site, so these can be considered irrelevant for binding. All C-termini were capped as amides and all N-termini as formamides, except the N-terminus of residue 21, which was capped as an acetamide because the resulting amide bond is in a suitable position to interact with the nearby dimethylamino moiety of TSA, thus necessitating a more accurate description of its electronic properties. This finally resulted in an active site model consisting of 322 atoms (1924 contracted gaussians for a 3-21G* basis set), depicted in Fig. 4.

Force relaxation of TSA in the active site model of HDLP

The positions of all atoms of the HDLP protein including the catalytic Zn^{2+} ion were fixed, except for the OH hydrogen atoms of Tyr 91 and Tyr 297, because their positions cannot unequivocally be derived from the X-ray structure, and an *ad hoc* placement of these atoms could greatly influence the electrostatical and sterical properties of the protein. Also, the N^{π} protons of His 131 and His 132 were not fixed to allow both the His–Asp charge relay systems in the active model to adapt during the course of the calculation; see Fig. 5.

No constraints were imposed on TSA itself. Following energy minimization, a proton transfer from TSA to His 131 was apparent: in the final conformation, TSA's hydroxamic acid proton was located closer to N^{τ} of His 131 (1.05 Å) than to the oxygen atom of TSA's hydroxamic acid function (1.77 Å). While HDLP is an atypical zinc protease, its active site displaying features of both metallo- and serine proteases,[24] this type of proton transfer was previously observed in a calculation by Cross *et al*[37] on TACE, a zinc proteinase with a "conventional" active site, and is in accordance with the increased acidity of the zinc-bound ligand that resulted from their calculations.

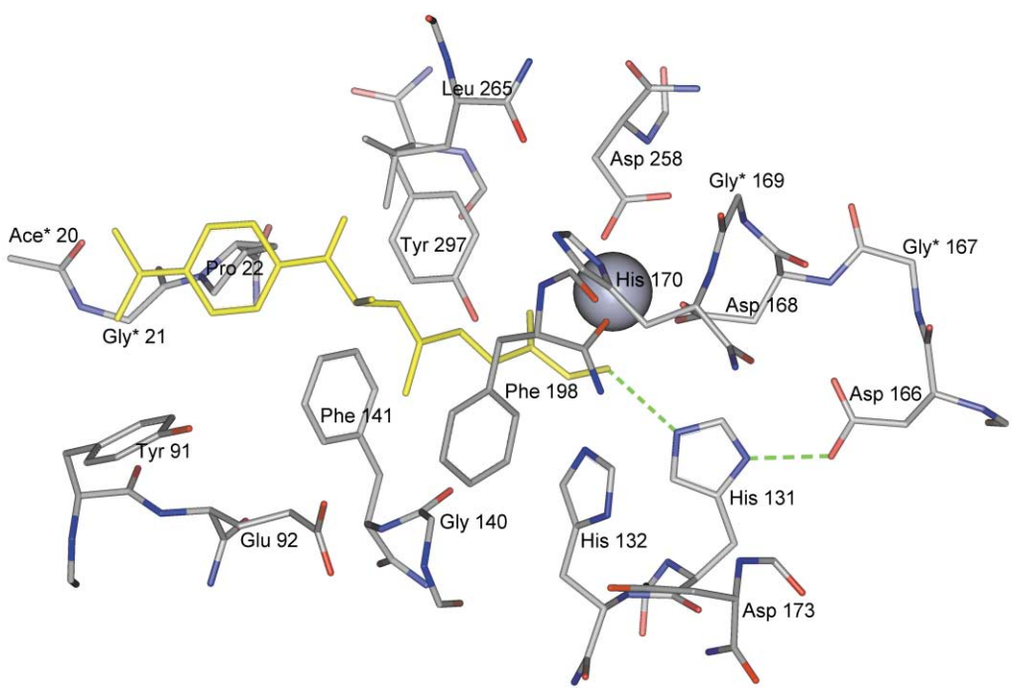

Fig. 4 The active site model, with bound TSA. Hydrogen atoms are omitted for clarity. The His131-Asp166 charge relay is marked; see Fig. 5 for its mechanism of action.

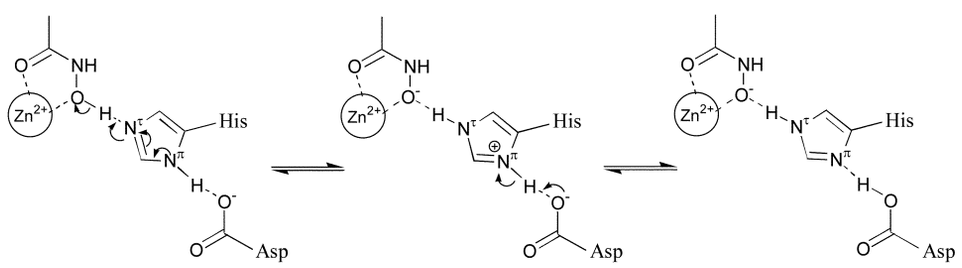

Fig. 5 The His–Asp charge relay system.

Force relaxation of water

Water was positioned in the active site with its oxygen atom at the same position as the hydroxamic acid OH oxygen atom, and with one of its hydrogen atoms pointing towards the N^{τ} atom of His 131. During the minimization, the geometry remained virtually the same. Because of the spontaneous deprotonation of TSA, a second minimization was started in which water was deprotonated by His 131 N^{τ}. In this minimization, the OH^- ion was displaced to the other side of the active site, near Tyr 297, as depicted in Fig. 6.

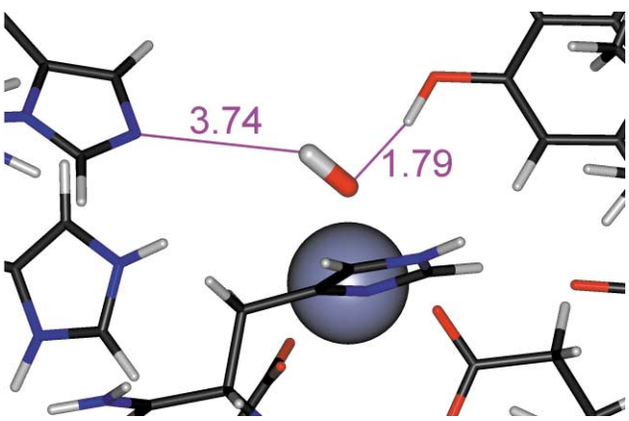

Fig. 6 Dissociated water in the HDLP active site.

The absolute energy of this structure was 16.8 kcal mol^{-1}‡ lower than the final energy of the previous minimization, thus indicating that water is deprotonated in the HDLP active site. Finally, as a test, Tyr 297 was deprotonated by the nearby OH^- ion and, starting from this structure, a third minimization was started. However, the resulting energy was 9.5 kcal mol^{-1} higher, confirming the final geometry of the second minimization as the most likely situation. Consequently, this geometry was be used for further BSSE calculations. The fact that water is deprotonated by His 131 confirms the first step of a proposed catalytic mechanism by Finnin *et al.*[24] However, the dissociation of water prior to eventual substrate binding and the subsequent displacement of the resulting OH^- ion to another location suggest that this mechanism involves a slightly different geometry than the one proposed.

Reference structures for the calculation of the binding energy

An estimate of the interaction energy in vacuum between the active site and the ligand in their respective final conformations can easily be calculated using BSSE correction. However, to make a meaningful estimate for the energy of binding, the energetic cost of bringing both systems in this binding conformation has to be included. For the protonated active site, the aforementioned Tyr OH hydrogen atoms, the His 131 and His 132 N^{π} protons and the His 131 N^{τ} proton were relaxed, in order to obtain a reference structure in which the same protons were allowed to move as in minimization of the HDLP-TSA complex. For TSA itself, a systematic conformational search was performed using the MMFF94 forcefield,[38] as included in the Sybyl software.[39] The conformation corresponding to the absolute minimum of this search was then further minimized at 3-21G* level. For reasons of consistency, water was also minimized at 3-21G* level.

BSSE corrected binding energy for TSA

The interaction energy was calculated using the counterpoise method for correcting the Basis Set Superposition Error, as explained in "theory and computational details". For TSA, this resulted in:

$$\begin{aligned}\Delta E_{binding} &= [E^{EL}_{bind}(EL) - E^{EL}_{bind}(E) - E^{EL}_{bind}(L)] + [E^{E}_{bind}(E) - E^{E}_{min}(E)] \\ &\quad + [E^{L}_{bind}(L) - E^{L}_{min}(L)] \\ &= -62.0 \text{ kcal mol}^{-1} + 9.1 \text{ kcal mol}^{-1} + 14.8 \text{ kcal mol}^{-1} \\ &= -38.0 \text{ kcal mol}^{-1}\end{aligned}$$

The magnitude of the first term is explained by the formation of a salt bridge between the negatively charged hydroxamic acid and the positive charges on Zn^{2+} and the histidine ring. The most significant contributions to the second term are probably the stretch of the His 131 N^{τ}–H bond and the transfer of this residue's N^{π} proton towards Asp 166. The third term is the conformational cost for deprotonated TSA to reach its binding conformation. Overall, the salt bridge provides the dominant contribution to the resulting energy of binding

In absolute value, the total energy of interaction is of the same order of magnitude as the experimental value for the Biotin-Streptavidin complex, −32 kcal mol^{-1}.[40] Since the latter is one of the higher-affinity noncovalent protein-ligand complexes described ($K_d = 3.9\ 10^{-14}$ M) and possibly the complex with the highest ΔH° reported, our result can be considered unlikely. However, as discussed below, comparison of this energy with the binding energy for water and inclusion of the deprotonation energies of TSA and water will produce a more realistic result.

BSSE corrected binding energy for water

The interaction energy was calculated in exactly the same way as described for TSA:

$$\begin{aligned}\Delta E_{binding} &= [E^{EL}_{bind}(EL) - E^{EL}_{bind}(E) - E^{EL}_{bind}(L)] + [E^{E}_{bind}(E) - E^{E}_{min}(E)] \\ &\quad + [E^{L}_{bind}(L) - E^{L}_{min}(L)] \\ &= -71.3 \text{ kcal mol}^{-1} + 7.9 \text{ kcal mol}^{-1} + 1.8 \text{ kcal mol}^{-1} \\ &= -61.6 \text{ kcal mol}^{-1}\end{aligned}$$

The values of the different terms can be explained using similar arguments as developed for TSA. In comparison with the case for TSA, the first term is lower when water is present in the active site. This may be attributed to the relative lack of steric hindrance between the ligand and the active site, the fact that OH^- has much more freedom to find an optimal position to chelate Zn^{2+}, and to the higher basicity of OH^-. The second term is comparable in magnitude with the case of TSA and the lower value for the third term is no surprise, given the fact that an OH^- ion has only one degree of conformational freedom. The higher total binding affinity for OH^- has to be interpreted with care, since the energy of deprotonation was not taken into account, which can be expected to be substantially higher for water than for an acidic ligand as TSA.

Total difference in binding energy between TSA and water

The energy of protonation was calculated using the counterpoise method to correct the Basis Set Superposition Error, as explained in "Theory and computational details". For TSA, this resulted in:

$$\begin{aligned}\Delta E_{prot} &= [E^{HB}_{HB}(HB) - E^{HB}_{HB}(B^-)] + [E_{HB^-}(B^-) - E_{B^-}(B^-)] \\ &= -390.9 \text{ kcal mol}^{-1} + 8.7 \text{ kcal mol}^{-1} \\ &= -382.2 \text{ kcal mol}^{-1}\end{aligned}$$

Analogously, the protonation energy for water was:

$$\begin{aligned}\Delta E_{prot} &= [E^{HB}_{HB}(HB) - E^{HB}_{HB}(B^-)] + [E_{HB^-}(B^-) - E_{B^-}(B^-)] \\ &= -425.7 \text{ kcal mol}^{-1} + 1.6 \text{ kcal mol}^{-1} \\ &= -424.1 \text{ kcal mol}^{-1}\end{aligned}$$

‡ 1 cal = 4.184 J.

Table 1 Changes in bond lengths for the mobile protons in the His–Asp charge relay systems

		Bond length/Å			
		Empty active site, deprotonated	Complex with TSA	Complex with water	Empty active site, protonated
His 131	N^{τ}–H	N/A [a]	1.048	1.008	1.005
	N^{π}–H	1.055	1.125	1.159	1.354
Asp 166	COO–H	1.439	1.367	1.332	1.137
His 132	N^{τ}–H	N/A [a]	1.654	N/A [a]	N/A [a]
	N^{π}–H	1.041	1.049	1.045	1.049
Asp 173	COO–H	1.787	1.779	1.783	1.779

[a] N/A: not available (the proton is not present in the given configuration).

The final expression for the difference in binding energy between TSA and water may thus be written as (see "theory and computational details"):

$$\Delta\Delta E_{tot} = \Delta E_{binding}(\mathrm{TSA}^-) - \Delta E_{prot}(TSA^-) - \Delta E_{binding}(OH^-) + \Delta E_{prot}(OH^-)$$
$$= -38.0 \text{ kcal mol}^{-1} + 382.2 \text{ kcal mol}^{-1} + 61.6 \text{ kcal mol}^{-1} - 424.1 \text{ kcal mol}^{-1}$$
$$= -18.3 \text{ kcal mol}^{-1}$$

The experimental pK_i value of 8.97 for the binding of TSA to mouse HDAC1,[20]§ corresponds to a ΔG_{bind} of -12.7 kcal mol^{-1}. This figure could be regained by adding a $-T\Delta S$ term of 5.6 kcal mol^{-1} to a ΔH value approximated as equal to our $\Delta\Delta E_{tot}$ value. Since this $-T\Delta S$ value is well within the range that can be expected for a protein-small molecule interaction[41] it can be concluded that our calculations resulted in a realistic energy of interaction.

Geometrical changes in TSA after energy minimization in the active site

The starting and final conformations are depicted in Fig. 7.

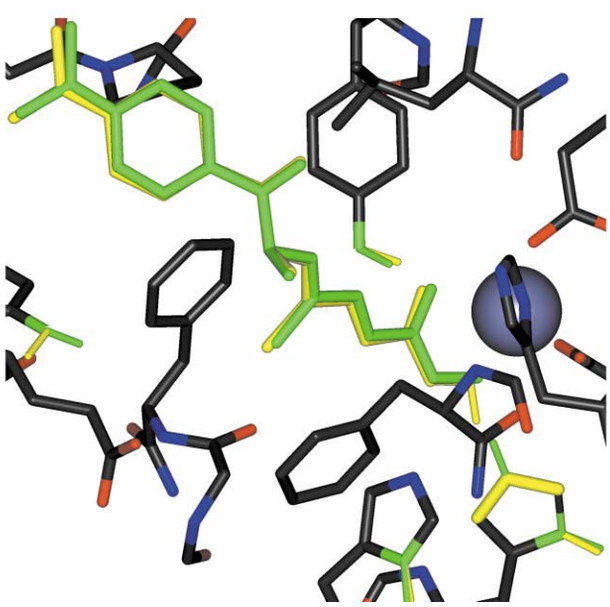

Fig. 7 Relaxation of TSA in the HDLP active site. The starting structure is colored yellow, the final structure green. Hydrogen atoms are omitted for clarity, except the hydroxamic acid proton and the two Tyr OH and His Nπ hydrogens. These hydrogen atoms are depicted by thinner sticks.

§ Mouse HDAC1 differs from human HDAC1 only in three residues, which are outside the region of homology between HDAC1 and the shorter protein HDLP. It can thus be concluded that HDLP is as similar to mouse HDAC1 as it is to human HDAC1 (35.2 % identity, as calculated by Finnin *et al.*)[24]

The RMSD between the non-hydrogen atoms of TSA in the X-ray structure versus the final structure of this calculation is 0.26 Å, so the result is in excellent accordance with this X-ray structure.

Geometrical changes in the active site

As mentioned before, the N^{π} protons of His 131 and His 132 were not fixed during the force relaxations in order to observe the proton displacements induced by the action of the His–Asp charge relay systems. The resulting bond lengths for the relevant protons in the minimized empty active site and complexes are listed in Table 1. For comparison, the empty active site was also deprotonated and minimized under the same conditions.

From these data, it can be concluded that, in comparison with the deprotonated active site, upon protonation of the N^{τ} atom of His 131 by TSA, the N^{π} proton moves 0.07 Å towards Asp 166, but can still be considered bound to His 131. To check whether this is not a metastable situation, the N^{π}–H bond length was set to 1.50 Å in the final structure of the minimization of TSA, yielding a COO–H bond length of 0.99 Å, and the structure was re-optimized starting from this point. However, this resulted in exactly the same conformation as before. In addition to excluding the possibility of a metastable situation, this finding indicates the absence of an energetic barrier to the displacement of this proton. Still, when the 3-21G* NH bond length of 1.001 Å in an isolated His^+ residue is compared with the His 131 N^{π}–H bond length of 1.367 Å in the complex, the latter appears considerably stretched.

All geometry-based conclusions regarding the His131–Asp 166 charge relay system in the HDLP-TSA complex are also valid for water, since the geometry of this charge relay system is similar. The N^{π} proton of His 131 was also released in a state bound to Asp 166 and also returned to its position bound to His 131. In comparison with TSA, this proton is 0.03 Å closer to Asp 166. This can be rationalized by the observation that the distance between the charge relay system and negative charge of the ligand is substantially larger with water.

Finally, in the protonated active site, the N^{π} proton of His 131 appears to be bound to Asp 166 rather than His 131. The fact that this proton transfer did not occur in the presence of an inhibitor can be explained by the polarizing effect of this ligand. The presence of a negatively charged group favors a polarized charge relay system, with a positively charged His close to the "external" negative charge and a negatively charged Asp further away, while in the absence of a site-bound anion, this charge separation may be less favorable. More specifically, the fact that this proton transfer did not occur in the HDLP–OH^- complex despite the relatively large distance of 7.49 Å between the negatively charged oxygen atom of this ligand and the N^{π} proton of His 131, indicates a high mobility of this proton, as could already be inferred from the absence of an energetic barrier to its displacement, and motivates the choice of an active site model that is relatively large for this type of calculations.

Table 2 Total charges and averaged atom-per-atom absolute deviations of Mulliken charges in different forms of the active site, compared to Mulliken charges in isolated His and Asp residues in different configurations, in a.u.

		Average absolute deviation [b]			RMSD [b]		
His 131 in [a]	Total charge [b]	$His^0(HN^\tau)$ [a]	$His^0(HN^\pi)$ [a]	His^+ [a]	$His^0(HN^\tau)$ [a]	$His^0(HN^\pi)$ [a]	His^+ [a]
$HDLP^0$	−0.563	0.127	0.056	0.126	0.155	0.061	0.151
$HDLP^+$-TSA^-	−0.364	0.106	0.121	0.059	0.139	0.150	0.073
$HDLP^+$-OH^-	−0.280	0.108	0.115	0.055	0.139	0.144	0.067
$HDLP^+$	−0.337	0.088	0.114	0.066	0.114	0.138	0.082
$His^0(HN^\tau)$	−0.403						
$His^0(HN^\pi)$	−0.414						
His^+	−0.149						

		Average absolute deviation [c]		RMSD [c]	
Asp 166 in [a]	Total charge [c]	Asp^- [a]	Asp^0 [a]	Asp^- [a]	Asp^0 [a]
$HDLP^0$	−0.644	0.010	0.069	0.011	0.078
$HDLP^+$-TSA^-	−0.637	0.016	0.066	0.018	0.071
$HDLP^+$-OH^-	−0.631	0.016	0.064	0.019	0.069
$HDLP^+$	−0.589	0.020	0.050	0.030	0.055
Asp^-	−0.644				
Asp^0	−0.438				

[a] $HDLP^0$: deprotonated active site, $HDLP^+$-TSA^-: TSA-bound active site, $HDLP^+$-OH^-: water-bound active site, $HDLP^+$: protonated active site, $His^0(HN^\tau)$: neutral isolated His residue with hydrogen on N^τ, $His^0(HN^\pi)$: neutral isolated His residue with hydrogen on N^π, His^+: protonated isolated His residue, Asp^-: deprotonated isolated Asp residue, Asp^0: neutral isolated Asp residue. [b] For all His residues, the complete imidazole ring was considered, but without eventual nitrogen-bound protons, to enable comparison between different configurations. [c] For the Asp residues, only the terminal carboxylate group was considered (C_γ and its two bound oxygen atoms).

Mulliken population analysis of the His131–Asp 166 charge relay system

To further investigate the nature of the bonds of the His 131 N^π proton to His 131 and Asp 166, Mulliken charges were generated for this charge relay system. The results can be found in Fig. 8.

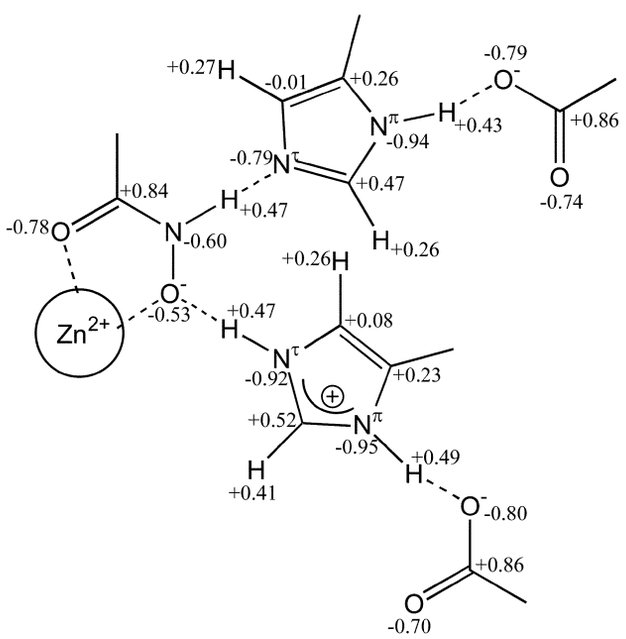

Fig. 8 Mulliken charges on the His–Asp charge relay systems, in *e*.

This exercise was repeated for the deprotonated active site, the protonated active site and the active site with bound water. The resulting charges in His 131 and Asp 166 were compared to 3-21G* Mulliken charges on isolated His and Asp residues: for each atom, the charge in the isolated residue was substracted from the charge in the active site. Then the absolute values of the resulting "charge deviations" were averaged over the relevant atoms in the residue. In the same way, RMSD's of the charges were calculated. The results of these calculations can be found in Table 2.

Clearly, the charges in the HDLP-TSA complex correspond much better with a protonated His^+ and a deprotonated Asp^- than with uncharged species, confirming the picture proposed in the section "Geometrical changes in the active site". Again, the same conclusion is also valid for water. However, in the protonated active site, the Mulliken charges in the charge relay system resemble those of a protonated His and a deprotonated Asp more than the charges on neutral species of these residues, thus contradicting the conclusion based on the geometry alone. Taking into account the elongated "covalent" bonds for the N^π proton, tabulated in Table 1, and the absence of an energetic barrier to the displacement of this proton, it seems reasonable to conclude that it should not be considered bound to either the His or the Asp residue, but exists in an intermediary situation. The high positive charge on this proton also points in this direction, being 0.49 *e* in the TSA-bound complex and 0.50 *e* in the water-bound complex and the protonated active site, compared to 0.42 *e* and 0.44 *e* for the acidic protons in an isolated Asp^0 and His^+ residue, respectively.

Conclusions

After the *ab initio* energy minimization of TSA in the active site of HDLP, a conformation was obtained that was in good agreement with the X-ray structure, lending credibility to the active site model used. Moreover the *ab initio* method clearly indicates, for the first time, a deprotonation of the hydroxamic acid by the His–Asp charge relay, a binding mechanism that cannot be demonstrated by molecular mechanics calculations. The observed deprotonation is in accordance with the increase in acidity of the zinc-bound ligand in zinc proteases calculated by Cross *et al.*[37] This deprotonation event, and the subsequent formation of salt bridges, explain the high potency of hydroxamic acids as HDAC inhibitor.

In the same way, water was minimized in the active site of HDLP. It was also deprotonated, confirming a possible catalytic mechanism that was proposed by Finnin *et al*,[24] based on its X-ray structure. However, the geometry of the final structure

of this minimization indicates that the catalytic mechanism has a slightly different geometry than the one proposed.

After the minimizations, an estimate of the binding energy was made. A realistic result was obtained, suggesting the methodology presented here may be used systematically in the future to compare the binding affinities of different inhibitors within a reasonable timespan.

In addition to the minimization of the protonated empty active site for determination of the binding energy, the deprotonated active site was minimized. The resulting geometries of the His 131–Asp 166 charge relay system were compared, together with the final structures of the abovementioned minimizations. From this, it can be concluded that the the N^{π} proton is still bound to the His residue upon protonation of N^{τ} by TSA, despite the strong effect of the Asp residue near the N^{π} proton of the His residue on its N^{τ} proton's acidity and the considerable elongation of the N^{π}–H bond. Although in the case of water, the distance of the negatively charged ligand to this charge relay system is considerably increased, thus decreasing its polarizing effect, the N^{π} proton can still be considered bound to the His residue. However, in the protonated active site devoid of any ligand, the N^{π} proton seems to be transferred to the Asp residue.

Mulliken charges on the His 131–Asp 166 charge relay system confirm the picture of a protonated His and deprotonated Asp residue for the TSA- and water-bound complexes, but suggest the situation is the same for the protonated active site, contradicting the conclusion based on its geometry. Together with the substantial elongation of the "covalent" bonds of the N^{π} proton in all positively charged His–Asp systems considered in this work, the absence of an energetic barrier to the displacement of this N^{π} proton, and the high positive charge on this proton, this leads to the conclusion that it is present in an intermediary situation between the state bound to His 131 and to Asp 166. This may in fact explain the ease of a His–Asp charge relay system to accept or release its N^{τ} proton "at will", with relatively low energetic barriers, a catalytically interesting property that accounts for the generous use of this motive in nature.

Acknowledgements

K. Vanommeslaeghe is a Research Assistant of the Fund for Scientific Research Flanders (Belgium)(F. W. O.-Vlaanderen). P. Geerlings also thanks the F. W. O.-Vlaanderen for continuous support of his research group.

References

1 P. T. Meinke and P. Liberator, *Curr. Med. Chem.*, 2001, **8**, 211–235.
2 P. A. Marks, V. M. Richon and R. A. Rifkind, *J. Natl. Cancer Inst.*, 2000, **92**, 1210–1216.
3 P. A. Marks, R. A. Rifkind, V. M. Richon, R. Breslow, T. Miller and W. K. Kelly, *Nat. Rev. Cancer*, 2001, **1**, 194–202.
4 D. M. Vigushin and R. C. Coombes, *Anti-Cancer Drugs*, 2002, **13**, 1–13.
5 K. Rombouts, T. Niki, P. Greenwel, A. Vandermonde, A. Wielant, K. Hellemans, P. De Bleser, M. Yoshida, D. Schuppan, M. Rojkind and A. Geerts, *Exp. Cell Res.*, 2002, **278**, 184–197.
6 T. Niki, K. Rombouts, P. De Bleser, K. De Smet, V. Rogiers, D. Schuppan, M. Yoshida, G. Gabbiani and A. Geerts, *Hepatology*, 1999, **29**, 858–867.
7 N. Mishra, D. R. Brown, I. M. Olorenshaw and G. M. Kammer, *Proc. Natl. Acad. Sci. USA*, 2001, **98**, 2628–2633.
8 F. Leoni, A. Zaliani, G. Bertolini, G. Porro, P. Pagani, P. Pozzi, G. Dona, G. Fossati, S. Sozzani, T. Azam, P. Bufler, G. Fantuzzi, I. Goncharov, S.-H. Kim, B. J. Pomerantz, L. L. Reznikov, B. Siegmund, C. A. Dinarello and P. Mascagni, *Proc. Natl. Acad. Sci. USA*, 2002, **99**, 2995–3000.
9 A. McCampbell, A. A. Taye, L. Whitty, E. Penney, J. S. Steffan and K. H. Fischbeck, *Proc. Natl. Acad. Sci. USA*, 2001, **98**, 15179–15184.
10 J. S. Steffan, S. Joan, L. Bodal, J. Pallos, M. Poelman, A. McCampbell, B. Apostol, A. Kazantsev, E. Schmidt, Y.-Z. Zhu, M. Greenwald, R. Kurokawa, D. E. Housman, G. R. Jackson, J. L. Marsh and L. M. Thompson, *Nature*, 2001, **413**, 739–743.
11 P. Papeleu, P. Loyer, T. Vanhaecke, G. Elaut, A. Geerts, C. Guguen-Guillouzo and V. Rogiers, *J. Hepatol.*, 2003, in press.
12 M. Yoshida, M. Kijima, M. Akita and T. Beppu, *J. Biol. Chem.*, 1990, **265**, 17174–17179.
13 K. Mori and K. Koseki, *Tetrahedron*, 1988, **44**, 6013–6020.
14 G. Elaut, G. Török, M. Vinken, G. Laus, P. Papeleu, D. Tourwé and V. Rogiers, *Drug Metab. Dispos.*, 2002, **30**, 1320–1328.
15 S. W. Remiszewski, L. C. Sambuchetti, P. Atadja, K. W. Bair, W. D. Cornell, M. A. Green, K. L. Howell, M. Jung, P. Kwon, N. Trogani and H. Walker, *J. Med. Chem.*, 2002, **45**, 753–757.
16 S. Singh, D. Zink, J. Polishook and A. Dombrowski, *Tetrahedron Lett.*, 1996, **37**, 8077–8080.
17 M. Kijima, M. Yoshida, K. Sugita, S. Horinouchi and T. Beppu, *J. Biol. Chem.*, 1993, **268**, 22429–22435.
18 V. M. Richon, Y. Webb, R. Merger, T. Sheppard, B. Jursic, L. Ngo, F. Civoli, R. Breslow, R. A. Rifkind and P. A. Marks, *Proc. Natl. Acad. Sci. USA*, 1996, **93**, 5705–5708.
19 S. Massa, A. Mai, G. Sbardella, M. Esposito, R. Ragno, P. Loidl and G. Brosh, *J. Med. Chem.*, 2001, **44**, 2069–2072.
20 A. Mai, S. Massa, R. Ragno, M. Esposito, G. Sbardella, G Nocca, R. Scatena, F. Jesacher, P. Loidl and G. Brosh, *J. Med. Chem.*, 2002, **45**, 1778–1784.
21 A. Mai, S. Massa, R. Ragno, I. Cerbara, F. Jesacher, P. Loidl and G. Brosh, *J. Med. Chem.*, 2003, **46**, 512–524.
22 R. Lavoie, G. Bouchain, S. Frechette, S. H. Woo, E. A. Khalil, S. Leit, M. Fournel, P. T. Yan, M.-C. Trachy-Bourget, C. Beaulieu, Z. Li, J. Besterman and D. Delorme, *Bioorg. Med. Chem. Lett.*, 2001, **11**, 2847–2850.
23 K. Vanommeslaeghe, G. Elaut, V. Brecx, P. Papeleu, K. Iterbeke, P. Geerlings, D. Tourwé and V. Rogiers, *Bioorg. Med. Chem. Lett.*, 2003, **13**, 1861–1864.
24 M. S. Finnin, J. R. Donigian, A. Cohen, V. M. Richon, R. A. Rifkind, P. A. Marks, R. Breslow and N. P. Pavletich, *Nature*, 1999, **401**, 188–193.
25 V. M. Richon, S. Emiliani, E. Verdin, Y. Webb, R. Breslow, R. A. Rifkind and P. A. Marks, *Proc. Natl. Acad. Sci. USA*, 1998, **95**, 3003–3007.
26 L. Qui, M. J. Kelso, C. Hansen, M. L. West, D. P. Fairlie and P. G. Parsons, *Br. J. Cancer*, 1999, **80**, 1252–1258.
27 P. Mignon, J. Steyaert, R. Loris, P. Geerlings and S. Loverix, *J. Biol. Chem.*, 2002, **277**, 36770–36774.
28 H. M. Berman, J. Westbrook, Z. Feng, G. Gilliland, T. N. Bhat, H. Weissig, I. N. Shindyalov and P. E. Bourne, *Nucl. Acids Res.*, 2000, **28**, 235–242.
29 Despite the fact that ESFF is developed for application on inorganic and organometallic molecules, it also is able to generate acceptable results, similar to CVFF, on organic compounds; see J. C. Martins, R. Willem and M. Biesemans, *J. Chem. Soc. Perkin Trans. 2*, 1999, 1513–1520.
30 Insight II version 98, Accelrys Inc. (Formerly MSI).
31 C. Van Alsenoy and A. Peeters, *J. Mol. Struct. (THEOCHEM)*, 1993, **105**, 19–34.
32 C. Van Alsenoy, *J. Comput. Chem.*, 1988, **9**, 620–626.
33 C. Van Alsenoy, C-H. Yu, A. Peeters, J. M. L. Martin and L. Schaefer, *J. Phys. Chem. A*, 1998, **102**, 2246–2251.
34 S. F. Boys and F. Bernardi, *Mol. Phys.*, 1970, **19**, 553; F. B. Van Duijneveldt, J. G. C. M. Van Duijneveldt – Van De Rijdt and J. H. Van Lenthe, *Chem. Rev.*, 1994, **94**, 1873–1885.
35 A. Szabo and N. S. Ostlund, in *Modern Quantum Chemistry*, McGraw-Hill Publishing Company, New York, 1989, Chapter 3.
36 D. L. Eng-Wilmot and D. Van Der Helm, *Acta Crystallogr., Sect. B*, 1981, **B37**, 718–721.
37 J. B. Cross, J. S. Duca, J. J. Kaminski and V. S. Madison, *J. Am. Chem. Soc.*, 2002, **124**, 11004–11007.
38 T. A. Halgren, *J. Comput. Chem.*, 1996, **17**, 490–519; T. A. Halgren, *J. Comput. Chem.*, 1996, **17**, 520–552; T. A. Halgren, *J. Comput. Chem.*, 1996, **17**, 553–586; T. A. Halgren and R. B. Nachbar, *J. Comput. Chem.*, 1996, **17**, 587–615; T. A. Halgren, *J. Comput. Chem.*, 1996, **17**, 616–641; T. A. Halgren, *J. Comput. Chem.*, 1999, **20**, 720–729; T. A. Halgren, *J. Comput. Chem.*, 1999, **20**, 730–748.
39 Sybyl 6.6, Tripos Inc.
40 P. C. Weber, J. J. Wendoloski, M. W. Pantoliano and F. R. Salemme, *J. Am. Chem. Soc.*, 1992, **114**, 3197–3200.
41 Some relevant examples of calorimetric studies on comparable systems that yield similar $T\Delta S$ terms are: S. M. Aitken, J. L. Turnbull, M. D. Percival and A. M. English, *Biochemistry*, 2001, **40**, 13980–13989; M. H. Parker, E. A. Lunney, D. F. Ortwine, A. G. Pavlovsky, C. Humblet and C. G. Brouillete, *Biochemistry*, 1999, **38**, 13592–13601.